Chapter 6

Classification of Faults using Vibro-Acoustic Sensor Data Fusion

This Chapter presents the novel technique for fault diagnosis of bearing by fusion of two different sensors: Vibration based and acoustic emission-based sensor. The diagnosis process involves the following steps: Data Acquisition and signal processing, Feature extraction, Classification of features, High-level data fusion and Decision making. Experiments are carried out upon test bearings with a fusion of sensors to obtain signals in time domain. Then, signal indicators for each signal have been calculated. Classifier called K-nearest neighbor (KNN) has been used for classification of fault conditions. Then, high-level sensor fusion was carried out to gain useful data for fault classification. The decision-making step allows understanding that vibration-based sensors are helpful in detecting inner race and outer race defect whereas the acoustic-based sensor is more useful for ball defects detection. These studies based on fusion helps to detect all the faults of rolling bearing at an early stage.

6.1 Introduction

Rolling element bearing is considered to be the most critical component of rotor-bearing systems. Condition monitoring of bearing is performed in industries like power, aerospace, manufacturing, etc. is a crucial preventive maintenance step to avoid catastrophic failures of machines due to defects occurring in bearing [1]. Thereby, early detection of faults is possible with the reliable health-monitoring scheme.

Traditionally, observing some of the condition-monitoring indices for maintenance activities is time-consuming, and it is not reliable when the data is noise affected. Vibration analysis has remained one of the most popular techniques of bearing health monitoring [2-4]. One of the major drawbacks of vibration analysis is non-detection of early bearing defects. Acoustic emission based health monitoring of bearing provides an alternative to overcome the drawback of vibration analysis [5-7]. Both these technique of bearing condition monitoring are very well known techniques with its advantages and disadvantages. Fusion of both the techniques into one system for health monitoring of

bearing may lead to the development of a reliable method of diagnosis and prognosis of rotary machines. Such a fusion overcomes the drawback of one technique over other technique of monitoring. Fusion of two different monitoring technique also leads to fusion of data, obtained from source signals of two transducers. Data fusion provides the most reliable fault-related information. Data availability in the form of important condition monitoring parameters, extracted from bearing signals, such as vibration and acoustic signals has motivated the use of data based fault diagnosis [8-9]. Data based fault diagnosis of the bearing is considered to be an automated intelligent diagnostics technique. Such a technique is in great demand in ultra-modern industries due to its accuracy and predicting capabilities of data [10]. Classical data based fault diagnosis techniques include statistical classifiers, polynomial classifiers and geometric methods [11]. These techniques may not be applicable for systems with time variation, because these models are dependent upon statistical parameters (Ex: RMS, Kurtosis, Skewness) obtained from vibration or acoustic data. Under automated diagnostic technique, decision based intelligent tools such as artificial neural network, fuzzy logic, expert system, genetic algorithm, neuro fuzzy, state observers, are widely used for rolling bearing fault diagnosis. Other than this tools, simpler machine learning algorithm such as support vector machines (SVM) and their associated models like K-nearest neighbor (K-NN) also are commonly used for fault detection and classification. SVM's and their related models are simple and easy to implement for various degrees of industrial applications [12]. Signal processing (SP)techniques such as wavelet transform(WT), short-time Fourier transform (STFT), and Hilbert-Huang transform (HHT) are also commonly used as a reliable source of health monitoring of rotating machinery. The major requirement of the SP technique in a signal analysis based condition monitoring is to remove carpet noise, speed fluctuations and smearing effects of vibration or acoustic signals. Although data-driven based techniques have been very well proposed and implemented for bearing fault diagnosis [13]. There is still a challenge to diagnose and classify the bearing faults based upon the data obtained from a single transducer. Since bearing posses a complex geometry with the inner race, outer race and number of rolling elements as its essential components. Localized defect occurring into multiple components of a bearing may not be accurately detectable by a single transducer. The diagnosis becomes difficult in the case of multiple-defects with information obtained

only from a single transducer. Such circumstances demand the paradigm shift into the new system, which must provide accurate diagnosis and classification of faults.

Over a few years, deep learning techniques are becoming a favorite tool for fault feature mining and smart diagnosis of rotating machinery with massive data. Li.et.al [14] performed fault detection of bearing by feeding FFT features as a pre-processor to the feed-forward neural network. Samanta and Al-balushi [15] developed the back propagation neural network for fault diagnosis with a reduced number of inputs for fewer iterations. In practice, measuring situations makes the neural network model very complicated . To overcome this complication, SVM proved to be the powerful technique of classification based on the statistical theory of learning, where results from training can be moved from one machine to another. Gryllias et al. [16] performed an automated diagnosis of defective bearing with proposed hybrid two stage one-against all SVM approach. Guo et al. [17] investigated the SVM method based on envelope analysis to diagnose rolling bearing with the faults on inner race, outer race and rolling elements. SVM's related model such as K-NN also performed well on classifying bearing fault conditions. M.S Safizadeh et al. [18] used K-NN classifier to identify the condition of ball bearing based on the data obtained from vibration and load signal. The capabilities of these machine learning classifiers have been tested with the data received from a single transducer. Integration of multiple diagnostic transducer data to classifier increases the reliability of the overall system. Fusion of multiple transducers used to acquire defect-related information provides accurate decision-making capabilities.

The objective here is to perform classification of bearing faults based on a combination of fault feature data obtained from the fusion of vibration and acoustic emission transducer. Here the fusion between these two sensors is named as vibro-acoustic fusion. Classification of the faults is performed by using the SVM model namely K-NN.

6.2 Experimental Test Rig and Measurement Condition.

Figure 6.1 depicts the experimental setup used in this study. Here the experimentations are carried out upon both defective and healthy bearing. The bearing of SKF ETN 9 1204 is

used for the study as mentioned in chapter (3). The defects are artificially seeded upon the surface of the bearing components using spark erosion technique. The accelerometer is mounted vertically on the top of the bearing housing, and acoustic emission microphone is placed with the help of attachment parallel to the housing. The orientation of both the sensors is shown in Figure 6.1.

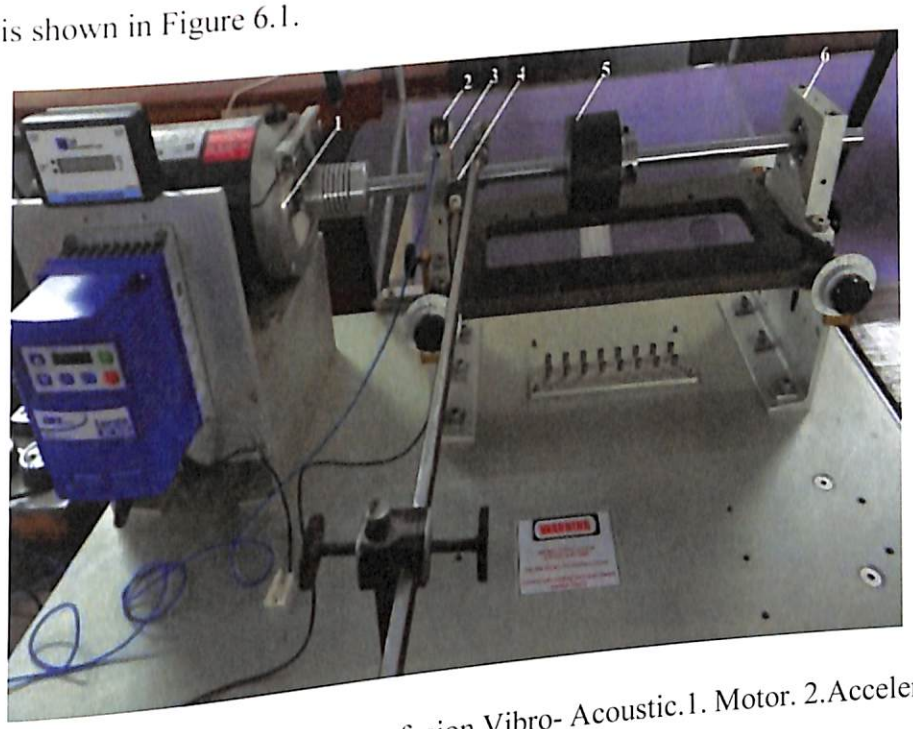

Figure6.1 Bearing Test rig with sensor fusion Vibro- Acoustic.1. Motor. 2.Accelerometer. 3.Defective bearing.4. Microphone (AE-Sensor).5. Bearing Loader.6. Healthy Bearing.

6.2.1 Instrumentations

Tri-axial accelerometer with a sensitivity of 102.0 mv/g was used for vibration measurements. The vibration response of accelerometer was using eight channels OR 35 real-time multi-analyzers. The multi-analyzer was connected to a computer with the help of network cable to obtain digital signals. Here acoustic emission sensor of specification 1/8" microphone type 40DD with a sensitivity of 0.65 mv/Pa was used as a second sensor.

The microphone was also connected to multi-analyzer along with an accelerometer. The schematic diagram of the instrumentations is shown in Figure 6.2.

6.2.2 Measuring Conditions

In this study, the measurement of vibration and acoustic signals were carried out for two speed conditions (700 and 1700 rpm), one loading condition (50 N) and three defect conditions on outer race (OR) and inner race (IR) and one defect condition on ball and combined defect (interaction between OR defect and ball, IR defect and ball). The conditions of bearings used in this study are shown in Table 6.1. Experimentations are carried out upon all the test bearings for mentioned conditions above. Sample photographs of the defects are shown in Figure 6.3. The number of conditions obtained by changing the speed and fault severity for both vibration and acoustic emission signals is shown in Table 6.2 and Table 6.3.

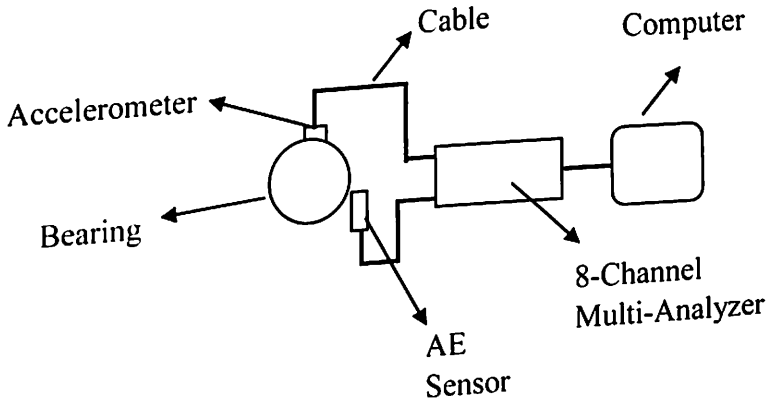

Figure 6.2 Schematic diagram of instrumentation.

6.3 Intelligent fault -diagnosis system

The flow chart of the proposed intelligent fault diagnosis system is shown in Figure 6.4. It consists of six basic module which combines to form the intelligent system to provide accurate fault diagnosis.

6.3.1 Data Acquisition and signal processing

Firstly, vibration and acoustic emission data were obtained from vibration sensor-accelerometer and acoustic emission sensor attached to the test bearing in its radial direction. The acquisition of signals has been made for 10 seconds, and these signals passed through inbuilt anti-aliasing filter of the analyzer.

(a)

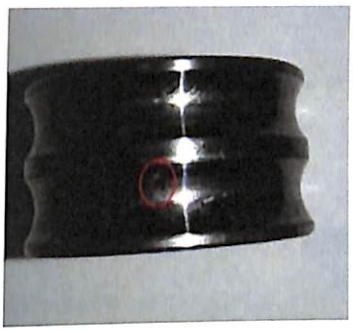

(b)

(c)

(d)

Figure 6.3 Sample Photographs of defects (a) Outer race defect (b) Inner race defect (c) Ball Defect (d) Combined defect.

Table 6.1 Conditions of bearing.

Fault Dimensions (L×W×D)	Faults Name
1.0×0.5×0.3	OR1, IR1
1.0×0.75×0.5	OR2, IR2
1.0×1.0×0.75	OR3, IR3
0.5×0.5×0.5	Ball Fault
0.5×0.5×0.5	Combined Defect (BDOR, BDIR)

6.3.1.1 Time Domain Analysis

Over the years, time domain analysis has been the potential signal processing method for bearing diagnosis. It is mainly based upon the demographic factors such as Kurtosis, Mean, RMS, Crest factor, skewness, etc. The correlation between vibration acceleration and bearing wear is very well shown by RMS value [12-13]. As the peakedness of the vibration increases, values of kurtosis and crest factors also increases.

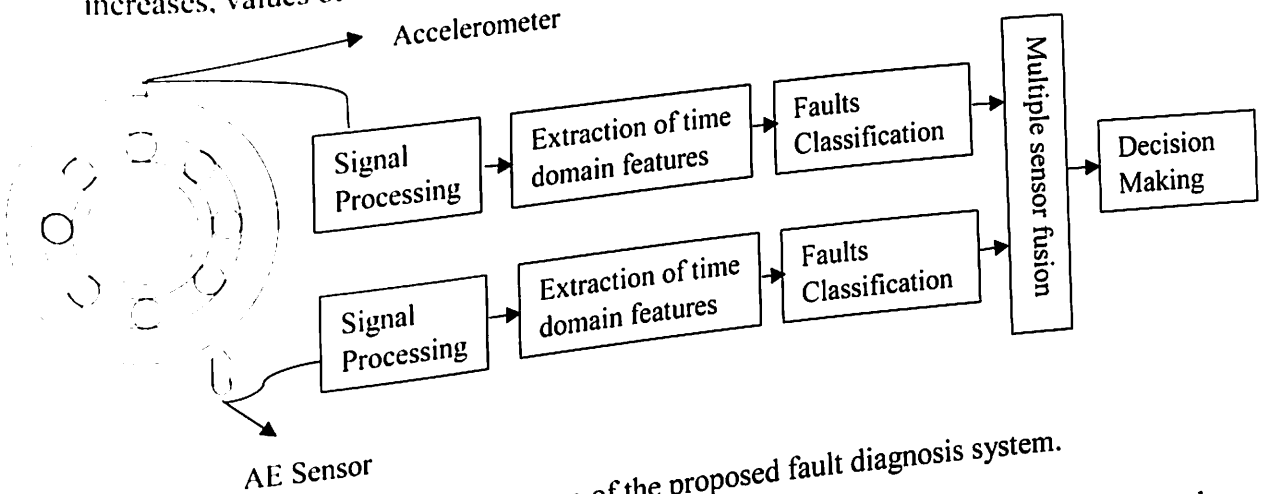

Figure 6.4 Flow diagram of the proposed fault diagnosis system.

In this way, kurtosis and crest factors are critical parameters to the shape of the signal. However, kurtosis is sensitive to the frequency bandwidth and rotational speed. The third central moment (skewness) is the poor measure of bearing fault features. The peak value of the vibration signal can be used as an indicator to defect condition, but it is not very useful when the defect is at the nascent stage. However, kurtosis was found to be efficient in narrow bands at high frequencies for incipient defects [19]. In this work, each vibration signal is processed to extract nine time-domain statistical parameters: maximum (M1), minimum (M2), standard deviation (M3), kurtosis (M4), skewness (M5), RMS (M6), Variance (M7), Peak2rms (M8) and median (M9). These parameters were used as input to the proposed intelligent fault diagnosis system.

6.3.2 Features Extraction

The features extraction process is implemented here to remove irrelevant variables from the features which may otherwise reduce the recognition accuracy of the classifier. At this point, time domain features are calculated for vibration and acoustic sensors. In this work,

principal component analysis (PCA) presented to select the appropriate features from the feature set, that can very well represent the fault features. PCA offers a subset of information, Contains the most significant information about the features, which thus reduces the dimension of the extensive feature set by eliminating the redundancy of data. PCA preserves the relevant fault related information into its subset when it is applied for fault diagnosis. In the PCA method, reduction of the dimensions performed by extracting the maximum variance from the variables of dimensions. Mathematically, PCA finds the eigenvectors to reflect both common and unique variance variables. Thus, PCA can be seen as a variance-focused approach. Here, the statistical parameters are treated as input to this module whereas defect conditions are treated as principal components for output [18].

6.3.3 Classification

Most of the intelligent fault diagnosis system for rotary machines uses a classification of the signal to obtain high accuracy and elimination of human error Recognition. In this work, K-nearest-neighbor (K-NN) has been applied for classification of bearing faults is one of the most straightforward algorithms that accumulates all present cases and classifies new instances based on a similarity measure (minimum distance). The process of K-NN is divided into two phases: the training set and the test phases. The training set trains the objects of different classes of interest. In the training phase, a model is constructed from the training instances, and the classification algorithm finds relationships between predictors and targets. In the testing phase, the model is tested based on a test sample whose class labels are known but not used for training the model. The K-NN uses standard Euclidean distance to find the nearest neighbors of an example. According to the value of K and the intervals, the classification of the sample is performed. The standard Euclidean distance equation for calculating the length of nearest neighbors is given by

$$d=\sqrt{\left(X_1^t - X_1^q\right)^2 + \left(X_2^t - X_2^q\right)^2} \quad (6.1)$$

where X_1^t, X_2^t denotes principal components of training points and X_1^q, X_2^q denotes testing points.

Table 6.2 Feature matrix of vibration sensor.

Class	Name	M1	M2	M3	M4	M5	M6	M7	M8	M9
1	H1-S1	1.89	-1.5028	0.2673	3.6275	-0.013	0.2673	0.0715	5.9479	-0.00017602
1	H1-S2	1.1647	-1.2641	0.239	3.1875	0.0146	0.239	0.0571	5.2898	-9.48E-04
1	H1-S3	2.2807	-2.8343	0.4966	3.1834	-0.0169	0.4966	0.2466	5.7074	-2.72E-05
1	H2-S4	4.2706	-4.1282	0.9901	3.1087	0.0024	0.9901	0.9803	4.3133	0.0115
2	OR1-S1	0.3658	-0.3525	0.0749	3.3177	-0.0157	0.0749	0.0056	4.8868	0.00042855
2	OR1-S2	0.5045	-0.552	0.1141	3.219	-0.0264	0.1141	0.013	4.8368	3.55E-04
2	OR1-S3	0.5856	-0.5385	0.129	3.1796	0.0583	0.129	0.0166	4.5403	2.94E-04
2	OR1-S4	2.2408	-2.6248	0.6476	3.0531	0.0226	0.6476	0.4193	4.0533	-0.0078
2	OR2-S1	1.3237	-1.1951	0.1227	4.7839	0.0129	0.1227	0.0151	10.7895	0.00027019
2	OR2-S2	0.906	-1.0013	0.1946	3.6327	0.0182	0.1946	0.0379	5.1454	-9.00E-04
2	OR2-S3	2.2624	-2.3542	0.3006	6.8604	0.037	0.3006	0.0903	7.833	1.90E-03
2	OR2-S4	2.7703	-2.8058	0.5733	3.2053	-0.0633	0.5733	0.3286	4.8943	-0.0041
2	OR3-S1	1.1883	-1.0671	0.1496	5.7695	-0.0348	0.1496	0.0224	7.945	0.00084768
2	OR3-S2	1.1135	-0.8556	0.1291	4.5745	0.0625	0.1291	0.0167	8.6256	-3.96E-04
2	OR3-S3	1.3042	-1.5264	0.3	3.406	-0.014	0.3	0.09	5.0877	-1.40E-03
2	OR3-S4	2.2844	-2.3454	0.4822	3.0048	0.027	0.4822	0.2325	4.8636	-0.011
3	IR1-S1	0.7819	-0.7317	0.1442	4.3277	-0.0196	0.1442	0.0208	5.4222	-0.000098113
3	IR1-S2	1.1088	-1.0188	0.1496	4.7452	-0.0135	0.1496	0.0224	7.41404	0.0021
3	IR1-S3	1.2089	-1.2146	0.2821	3.0611	0.078	0.2821	0.0796	4.3051	-0.0036
3	IR1-S4	3.4455	-3.257	0.8375	3.316	0.2266	0.8375	0.7014	4.114	-0.0334
3	IR2-S1	1.0961	-1.135	0.2269	3.9811	-0.102	0.2269	0.0515	5.0032	0.0026
3	IR2-S2	1.6437	-1.7799	0.3187	4.7512	-0.1395	0.3187	0.1016	5.5847	0.0013
3	IR2-S3	1.6631	-1.62	0.3743	3.8286	-0.0254	0.3743	0.1401	4.4433	0.0014
3	IR2-S4	2.3082	-2.002	0.507	3.0131	0.2248	0.507	0.257	4.5528	-0.027
3	IR3-S1	1.5851	-1.9395	0.287	8.0358	-0.2652	0.287	0.0824	6.7577	-0.0012
3	IR3-S2	2.4432	-3.0319	0.3438	14.5811	-0.3614	0.3438	0.1182	8.8196	0.0043
3	IR3-S3	2.7218	-3.2639	0.5651	5.5661	-0.0631	0.5651	0.3193	5.7758	-0.0094
3	IR3-S4	3.057	-3.1159	0.6205	4.3498	-0.1696	0.6205	0.385	5.0216	0.0162
4	BD-S1	86.7571	-59.7623	19.5269	5.2268	1.282	20.3218	381.3017	4.2692	-11.34
4	BD-S2	79.4042	-29.3122	13.8268	7.8391	1.9976	13.827	191.1804	5.7427	-5.1948
4	BD-S3	14.2373	-56.601	2.8443	33.3535	-2.2154	2.8616	8.0898	19.7798	0.0914
4	BD-S4	14.2383	-64.9771	3.4576	25.1333	-1.4454	3.4927	11.9549	18.6038	-1.0912
5	BDIR-S1	96.4041	-31.7367	12.1883	11.5504	2.189	12.4231	148.5554	7.7601	-0.4822
5	BDIR-S2	68.5975	-49.9118	16.9626	4.5244	1.2236	16.9764	287.7299	4.0408	-4.4041
5	BDIR-S3	13.2913	-79.1652	3.5243	18.531	-1.1562	4.6267	12.4208	17.1104	-3.2059
5	BDIR-S4	9.8197	-49.7325	1.9815	44.8857	-2.7201	2.1132	3.9265	23.5341	-0.797
6	BDOR-S1	69.2213	-32.4379	14.8195	5.5908	1.5505	15.0271	219.618	4.6064	-7.1882
6	BDOR-S2	75.6626	-51.8443	17.2547	5.158	1.3055	1.3055	297.7237	4.3837	-3.3303
6	BDOR-S3	19.3163	-74.6814	4.366	22.5269	-1.2815	4.3782	19.0619	17.0576	-0.5103
6	BDOR-S4	11.3066	-47.9495	2.6739	42.8491	-3.3562	-3.3562	7.1499	17.7803	-0.3589

Classification borders are obtained for both sensors by using equation (6.1) which are as shown in Figure 6.5

6.3.4 Multiple sensor fusion

The process of fusion of information, obtained from different sensors, is known as multiple sensor fusion. In this paper, two different sensors are used for collecting fault related information of bearing. These sensors are an accelerometer and acoustic emission sensor. Multiple sensor fusion can be performed at three levels: data level, feature level, and decision level.

- Data level fusion

The raw data recorded by different sensors from machinery are directly combined to produce more relevant, informative data than the original data generated by each sensor. Then, the combined data undergoes feature extraction process followed by a pattern recognition process for the classification of faults. At this stage, fused data is more efficient and reliable for diagnostic than the data obtained from an individual sensor. However, data fusion is performed upon the data collected for the same physical parameters or quantities, measured by each sensor. Hence, application of data-level fusion is limited to the data from the corresponding sensor.

Table 6.3 Feature Matrix of Acoustic Sensor.

Class	Name	M1	M2	M3	M4	M5	M6	M7	M8	M9
1	H1-S1	1.5944	-1.4785	0.4042	2.8456	0.2082	0.4042	0.1634	3.9442	-0.0143
1	H1-S2	0.0011	-0.0011	2.97E-04	2.9039	0.0326	2.97E-04	8.82E-08	3.8247	-7.33E-06
1	H1-S3	1.8038	-1.6172	5.02E-01	2.9024	0.1857	5.02E-01	2.52E-01	3.5911	-2.42E-02
1	H2-S4	0.0075	-0.0083	0.0023	2.5316	0.3853	0.0023	5.41E-06	3.5758	-3.01E-04
2	OR1-S1	0.4143	-0.4824	0.1195	2.9355	0.0089	0.1198	1.43E-02	4.0255	-8.50E-03
2	OR1-S2	8.07E-04	-9.85E-04	2.72E-04	2.5121	-0.2414	2.72E-04	7.41E-08	3.6193	1.49E-05
2	OR1-S3	9.26E-01	-1.15E+00	3.08E-01	2.623	-0.4304	3.08E-01	9.50E-02	3.7437	3.90E-02
2	OR1-S4	0.0059	-0.0052	0.0026	1.7998	0.0581	0.0026	6.63E-06	2.2959	-2.49E-04
2	OR2-S1	1.3671	-1.0489	0.2675	3.3258	0.0896	0.2678	7.16E-02	5.1039	-1.43E-02
2	OR2-S2	9.48E-04	-0.001	2.51E-04	3.0543	-0.0113	2.51E-04	6.30E-08	4.0408	3.87E-06
2	OR2-S3	1.36E+00	-1.316	4.20E-01	2.5016	0.0245	4.20E-01	1.77E-01	3.2303	8.20E-03
2	OR2-S4	0.0056	-0.0052	0.0024	2.0006	0.0891	0.0024	5.55E-06	2.3599	3.13E-06
2	OR3-S1	0.8519	-1.1081	0.2426	3.0532	-0.1398	0.2429	5.88E-02	4.5612	-9.20E-03
2	OR3-S2	9.77E-04	-8.83E-04	2.05E-04	3.1736	0.2296	2.05E-04	4.21E-08	4.7609	-1.47E-05
2	OR3-S3	1.46E+00	-1.57E+00	5.14E-01	2.5103	-0.1171	5.14E-01	2.64E-01	3.0489	1.53E-02
2	OR3-S4	0.0066	-0.0053	0.0026	2.0507	0.2138	0.0026	6.67E-06	2.5389	-4.54E-05
3	IR1-S1	1.1168	-1.1209	0.2815	2.9399	-0.0544	0.2817	7.93E-02	3.9792	1.23E-02
3	IR1-S2	9.79E-04	-8.25E-04	2.40E-04	3.0093	0.2374	2.40E-04	5.75E-08	4.083	-1.69E-05
3	IR1-S3	3.12E+00	-3.24E+00	5.30E-01	5.0355	-0.2117	5.30E-01	2.81E-01	6.1085	6.40E-03
3	IR1-S4	0.008	-0.0064	0.0028	2.3391	0.3072	0.0028	8.02E-06	2.8191	-3.81E-04
3	IR2-S1	1.4794	-1.2239	0.3093	2.89	0.0065	0.3093	9.56E-02	4.7826	-7.00E-03
3	IR2-S2	7.09E-04	-7.81E-04	1.85E-04	2.9054	-0.0735	1.85E-04	3.41E-08	4.2321	-1.33E-06
3	IR2-S3	1.62E+00	-1.39E+00	4.12E-01	3.0492	0.2183	4.12E-01	1.69E-01	3.9271	-1.14E-02
3	IR2-S4	0.0053	-0.0052	0.0022	1.9927	0.0666	0.0022	4.83E-06	2.4029	1.59E-04
3	IR3-S1	1.3073	-1.0975	0.2927	2.9135	0.0501	0.2928	8.57E-02	4.6707	-3.90E-03
3	IR3-S2	0.0011	-9.59E-04	2.08E-04	3.4285	-0.048	2.08E-04	4.33E-08	5.3817	-6.98E-06
3	IR3-S3	1.8316	-2.00E+00	6.50E-01	2.2117	-0.0788	6.50E-01	4.22E-01	3.071	2.00E-03
3	IR3-S4	0.0059	-0.0056	0.0024	2.0151	0.1575	0.0024	5.86E-06	2.4469	-3.51E-05
4	BD-S1	2.9576	-23.9464	3.1196	10.0593	-2.6055	3.1308	9.73E+00	7.6487	9.94E-01
4	BD-S2	0.0012	-0.0013	2.86E-04	3.0085	-0.0641	2.86E-04	8.18E-08	4.56	-3.90E-06
4	BD-S3	10.9175	-38.538	6.14E+00	3.0599	-0.5745	6.20E+0	3.77E+01	6.2195	5.20E-03
4	BD-S4	0.0158	-0.0426	0.0074	4.1773	-1.145	0.0074	5.41E-05	5.7193	0.0029
5	BDIR-S1	1.195	-1.9286	0.2872	5.0805	-0.6892	0.2872	8.25E-02	6.7148	0.0096
5	BDIR-S2	0.003	-0.0201	0.0022	5.9676	-1.666	0.0024	5.05E-06	8.531	-1.39E-04
5	BDIR-S3	11.6272	-61.7625	5.8134	4.4941	-1.1784	6.3922	3.38E+01	9.6624	4.32E+00
5	BDIR-S4	0.013	-0.0404	0.0047	2.7917	-0.3078	0.0048	2.23E-05	8.3793	0.0013
6	BDOR-S1	1.351	-1.0671	0.2641	3.2349	0.1963	0.338	6.98E-02	3.9974	0.1943
6	BDOR-S2	0.0066	-0.0115	0.0023	2.4831	0.046	0.0024	5.30E-06	4.8015	6.16E-04
6	BDOR-S3	14.0442	-57.8465	9.5443	2.9594	-0.6392	9.5472	9.11E+01	6.059	5.08E-01
6	BDOR-S4	0.011	-0.0359	0.0051	3.0972	-0.4669	0.0055	2.56E-05	6.5211	-0.0017

- Feature -Level fusion

In this level, the features extracted by applying signal processing techniques from different sensors are combined. Feature-level fusion is considered to be an intermediate level of the fusion process that involves a combination of features from non-commensurate sensors. Then, all elements are combined to obtain optimal features subset, which is then fed into the classifier.

- Decision-level Fusion

Decision level fusion is the highest level of fusion among all fusions. At this level of fusion, the decision is made based upon the fusion of results obtained from different sensors. This level of fusion enhances the importance of classifier combination to secure a decisive result. It also reduces the rate of misclassification regarding both false positives and false negatives [18]. The above-described models are based on the application of sensor fusion. However, there is not a local model for sensor data fusion. In this study, the fusion process was accomplished by an architecture known as waterfall fusion process model. This model was proposed by the defense department of Great Britain, in the year 1997. The steps involved in the process are as follows: (a) Sensing and signal processing corresponding to the sensor (b) Feature extraction and pattern recognition (c) Assessment of situation and decision making which corresponds to refinement of threat. The waterfall fusion process model is more accurate in analyzing the process of fusion compared to other models, but the major disadvantage of this model is the elimination of any feedback system.

Table 6.4 Effectiveness of each Technique.

Bearing Condition	**Vibration**	**Acoustic**	**Data Fusion**
Healthy	Healthy	Healthy	Healthy
OR1, IR1	OR1, OR2	Ball Fault	OR1, IR1
OR2, IR2	IR1, IR2	BDOR	OR2, IR2
OR3, IR3	OR3, IR3	BDIR	OR3, IR3
Ball Fault	OR1, IR1	OR	Ball Fault
BDOR, BDIR	OR2, IR2	Ball Fault	BDOR, BDIR

6.3.5 Decision making.

In this study, K-NNs are used for classifying faults. In K-NN, we consider each of the characteristics in the training set as a different dimension in some space and take the value an observation has for this characteristic to be its co-ordinate in that dimension, so getting a set of points in space. We can then consider the similarity of two points to be the distance between them in this space under some appropriate metric. The distance between the data points is calculated using distance function. The various distance functions available in K-NN are Euclidean, Manhattan, Mahalanobis, etc. In this work Euclidean distance function as described earlier is used to calculate the distance between data points for its similarities. Higher intervals indicate higher dissimilarities. The advantage of using Euclidean distance as a similarity measure is that many data points with the same class are close to each other according to distance measure in many local areas. The way the algorithm decides which of the points from the training set are similar enough to be considered when choosing the class to predict for a new observation or fault is the selection of cardinality function 'K' closest data points to the original comments, and to take the most common class among these. This is why it is known as the K-NN algorithm. Higher values of K provide less adaptive models and vice-versa. The output of the decision-making module provides the basis for corrective maintenance actions. The information provided to this module should diagnose faults of bearing and provides the classification of bearing faults.

6.4 Results and Discussions

Six different classes have been identified for training classifier: The Healthy condition of bearing, faults on the outer raceway, faults on the inner raceway, ball fault, ball fault and outer raceway fault and ball fault and inner raceway fault. Forty conditions of vibration and acoustic emission signals with various conditions of the severity of fault, constant loading condition, and different rotating frequency have been fed into an intelligent system of fault diagnosis during the training phase. Then, training data used by the classifier provides the boundaries of decision for the individual sensor, as shown in Figure 6.5(a) and Figure 6.5(b). The points of the decision boundaries are resulted by applying principal component analysis upon feature matrix in which rows corresponds to feature vectors. Here each feature vectors consists of nine signal features. The feature matrix of the

accelerometer and acoustic emission signals are presented in Table 6.2 and Table 6.3. The specification of the sensors plays an essential role in detecting the health state of the bearing. From the training results, it has been determined that accelerometer is robust in detecting the healthy state of bearing, outer race fault, and inner race fault but it is not very useful in identifying the actual fault condition caused by ball fault and its interaction with outer race fault and inner race fault. In its simplest form, the accelerometer is not so useful in determining the multiple faults. It is due to the high amplitude of vibrations caused by the multiple failures, which propagates to the housing of bearing, where the accelerometer is attached. Thereby, this accelerometer experiences large dynamic forces which affect its sensitivity and reduces its accuracy in determining the fault-related characteristics caused by the multiple faults. It is evident from Figure 6.5(b); acoustic emission technique provides effective detection of the ball fault and its interaction with both the raceways. From the Figure 6.5(b), it can be understood that there is a common boundary between the points of single fault and multiple faults. Thus, it can be easily inferred that acoustic emission classifies multiple defects along with a single fault. The boundaries in between the points of the accelerometer sensor are very indefinite from boundaries in between the ends of acoustic emission sensor. To develop fused data, feature matrix, four signals from acceleration and four signals from acoustic emission is taken into consideration. Then the fused data feature matrix is used to evaluate the performance of the proposed model.

Table 6.4 represents the actual bearing conditions and defect conditions assigned to each bearing by the accelerometer, acoustic emission, and data fusion. As observed in Table 6.4, condition monitoring only by accelerometer gives three false answers. It is evident that acoustic emission is a highly effective technique to detect ball fault and multiple faults. Meanwhile, condition monitoring by the accelerometer is very sensitive in detecting inner and outer race fault than its ball fault and multiple faults counterpart. However, the best performance in detection is observed from the fusion of data of both sensors. From Figure 6.5(c), the fusion of data classified all the faults within one boundary, thus making it easier to understand the classification of various faults. Figure 6.5(c) organized each fault closest to its neighboring fault, thus making it easy to classify the fault in its classes. The significant factor of the classification process is its visual representation also (Figure 6.5).

To help classification process having a visual image, here it is considered that the extractor module feeds only two features into the classifier.

Among the results of three cases, data fusion of both sensors proved to be effective in providing much more relevant information, than information obtained from an individual sensor. Multi-sensor fusion technique increases reliability, accuracy, and robustness in condition monitoring of bearing.

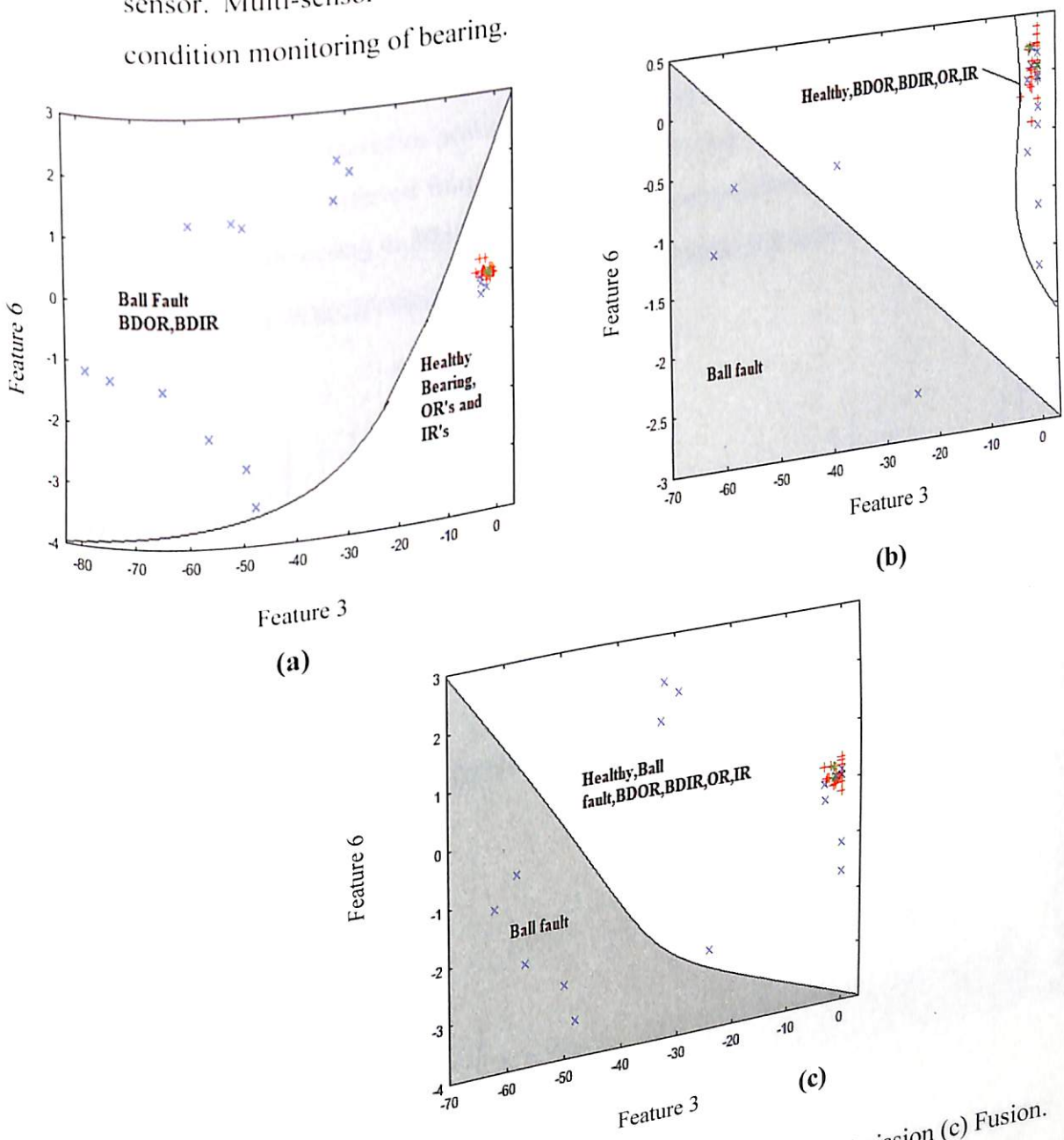

Figure 6.5. KNN Class borders illustration (a) Vibration (b) Acoustic Emission (c) Fusion.

6.4.1 Vibro-Acoustic FFT Results.

The Vibro-Acoustic FFT results are obtained for all the conditions of bearing mentioned in Table 6.1 at both speed condition i.e 700 r.p.m and 1700 r.p.m. The FFT results clearly states that Acoustic emission-based technique for fault detection is highly effective in detecting ball faults and multiple faults (Figures: - 6.8,6.9,6.10). In Figure 6.8, clear peaks can be observed in FFT of AE corresponding to the characteristic defect frequency of ball fault than the flat peaks present in FFT of accelerometer. Similarly, in Figure 6.9 &6.10, clear fault characteristics peaks are observed in FFT of AE than the FFT of accelerometer. Thus, it can be inferred from the results of FFT, that AE proved to be highly significant method in detecting multiple faults of rolling element bearings.

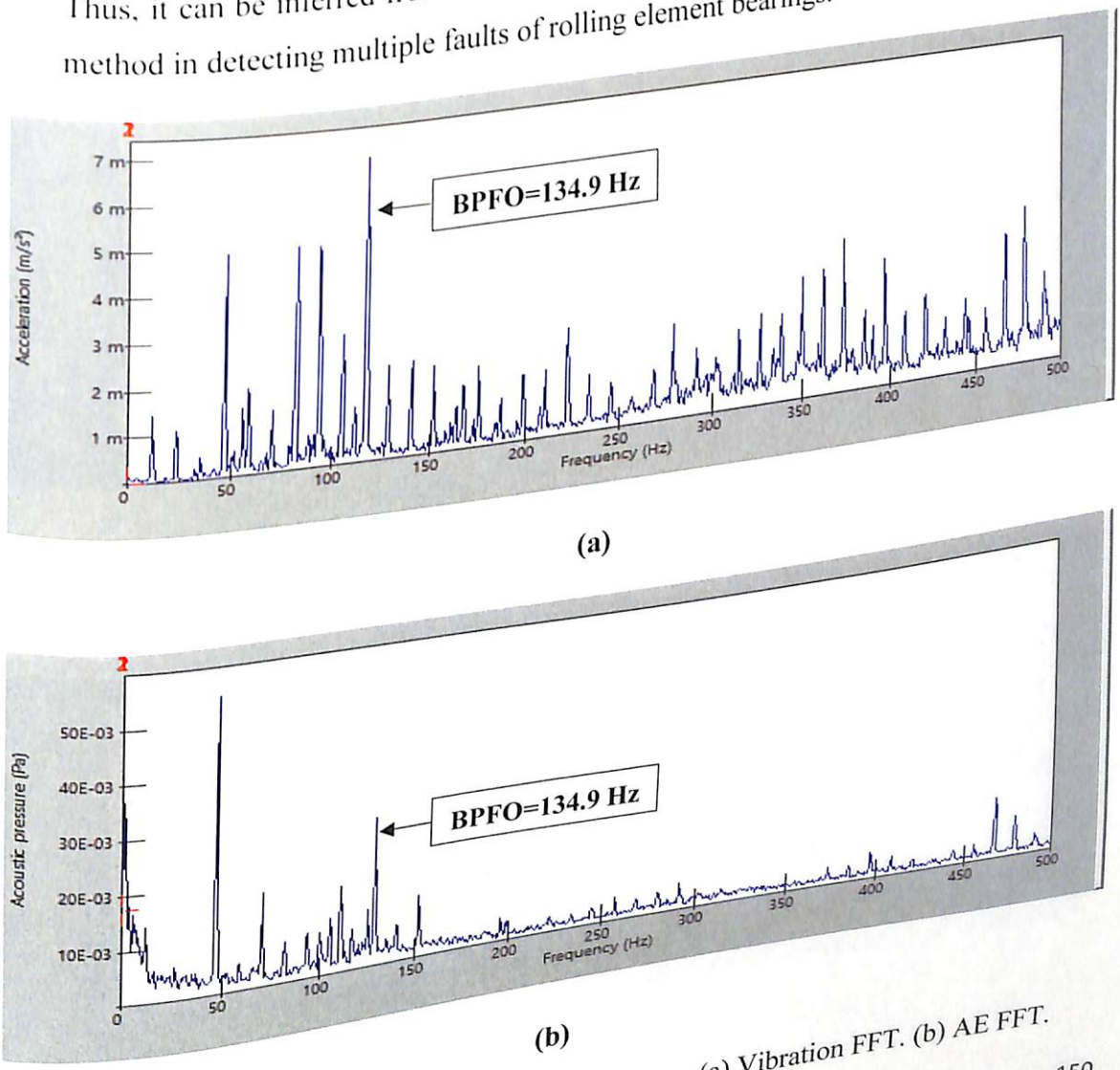

Figure 6.6 Vibro-Acoustic FFT of OR1 at 1700 rpm. (a) Vibration FFT. (b) AE FFT.

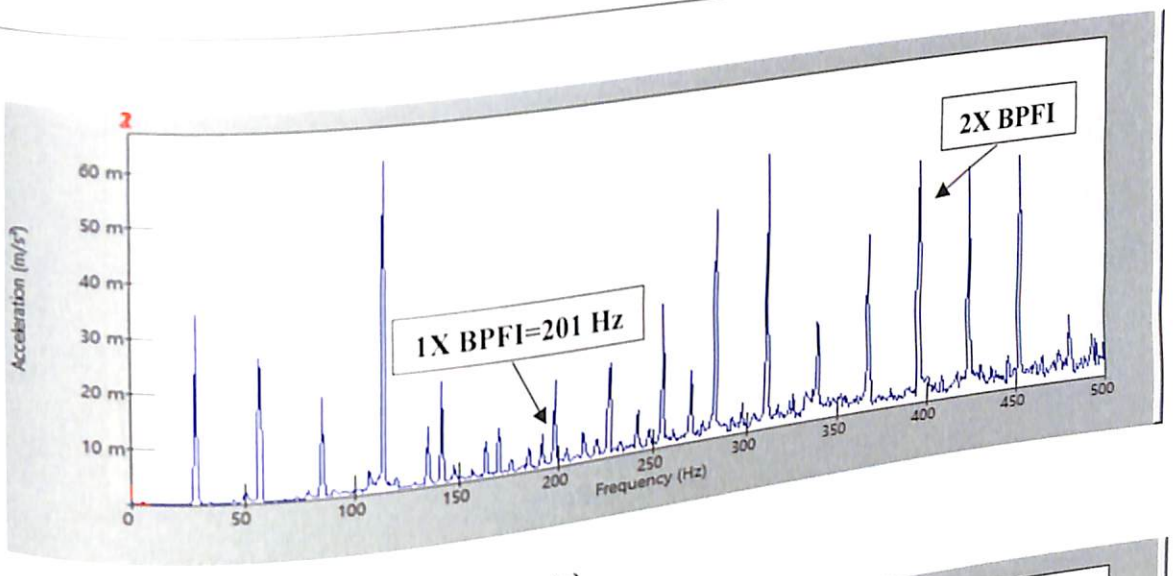

(a)

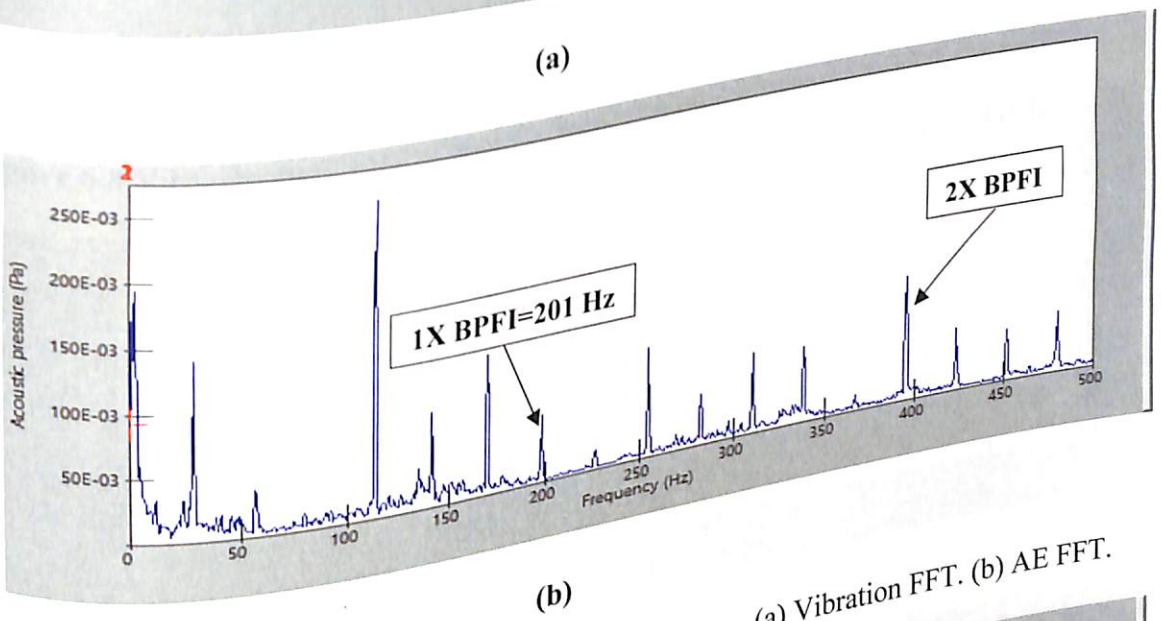

(b)

Figure 6.7 Vibro-Acoustic FFT of IR 1 at 1700 rpm. (a) Vibration FFT. (b) AE FFT.

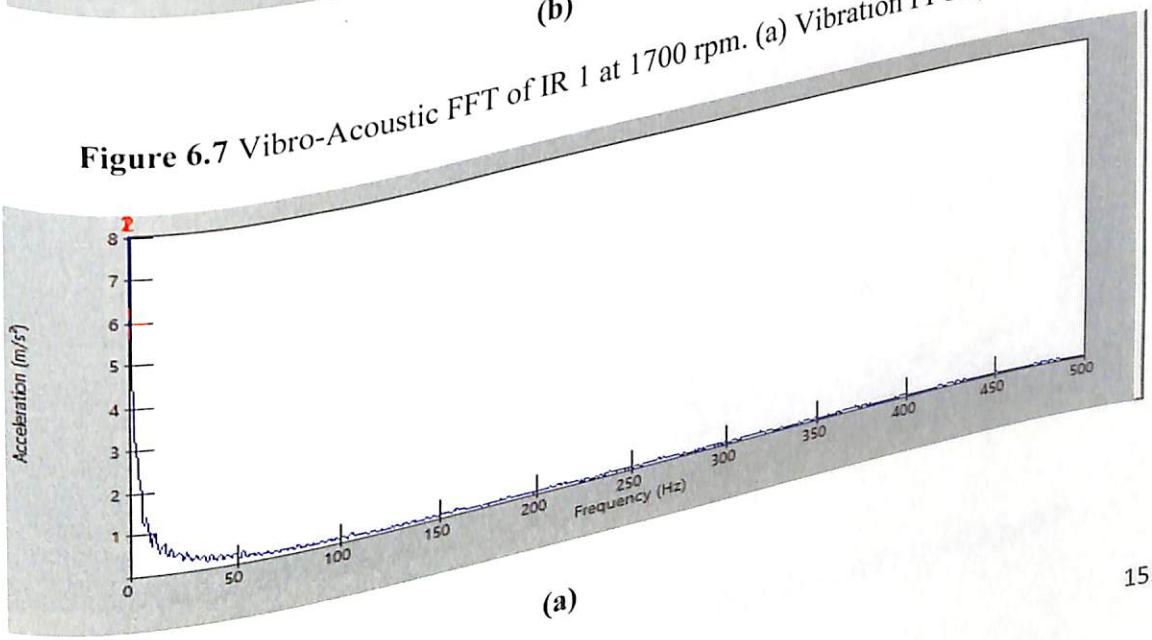

(a)

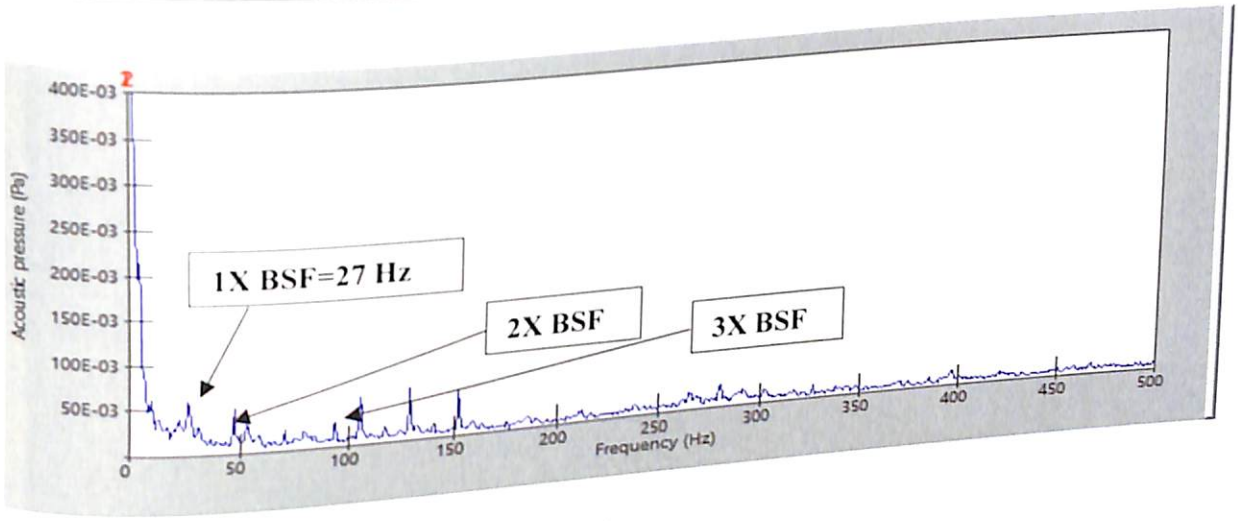

(b)

Figure 6.8 Vibro-acoustic FFT of Ball Defect at 700 rpm. (a) Vibration FFT. (b) AE FFT.

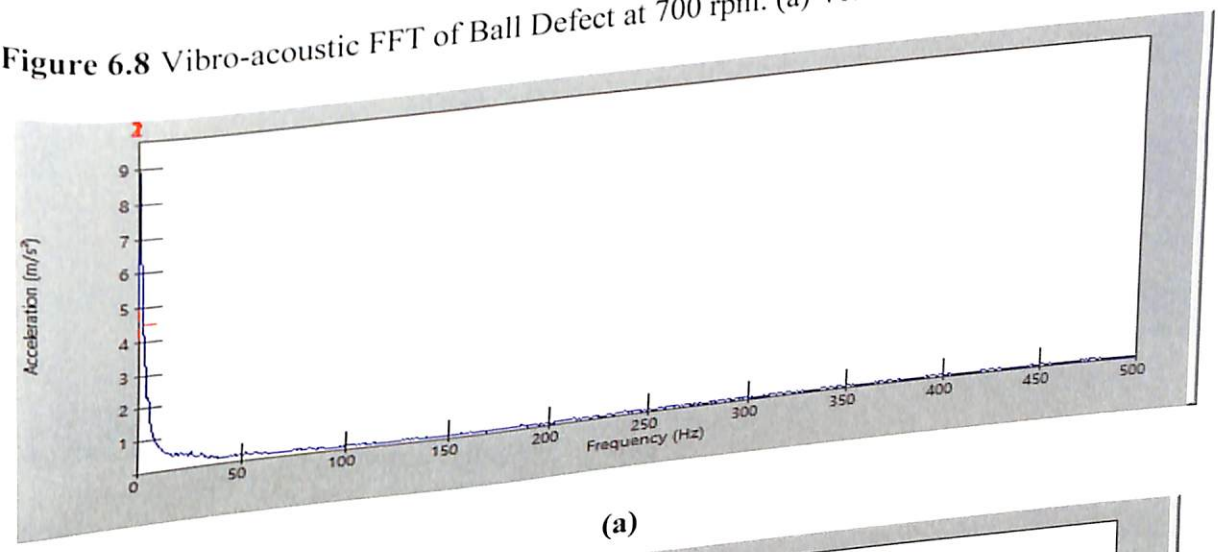

(a)

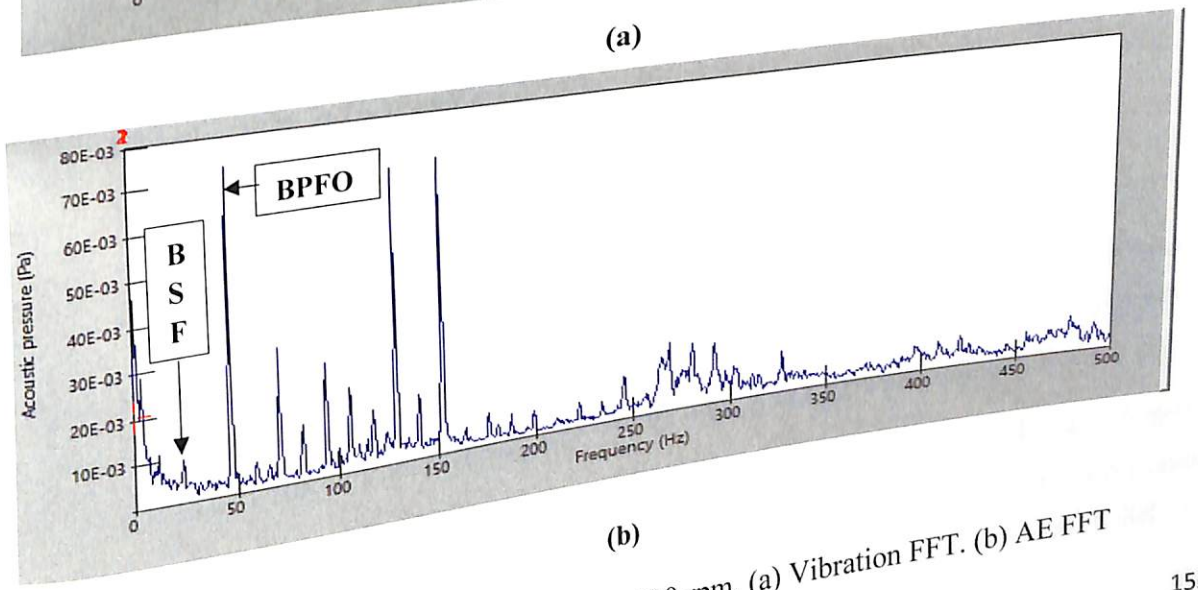

(b)

Figure 6.9 FFT of Ball and OR defect at700 rpm. (a) Vibration FFT. (b) AE FFT

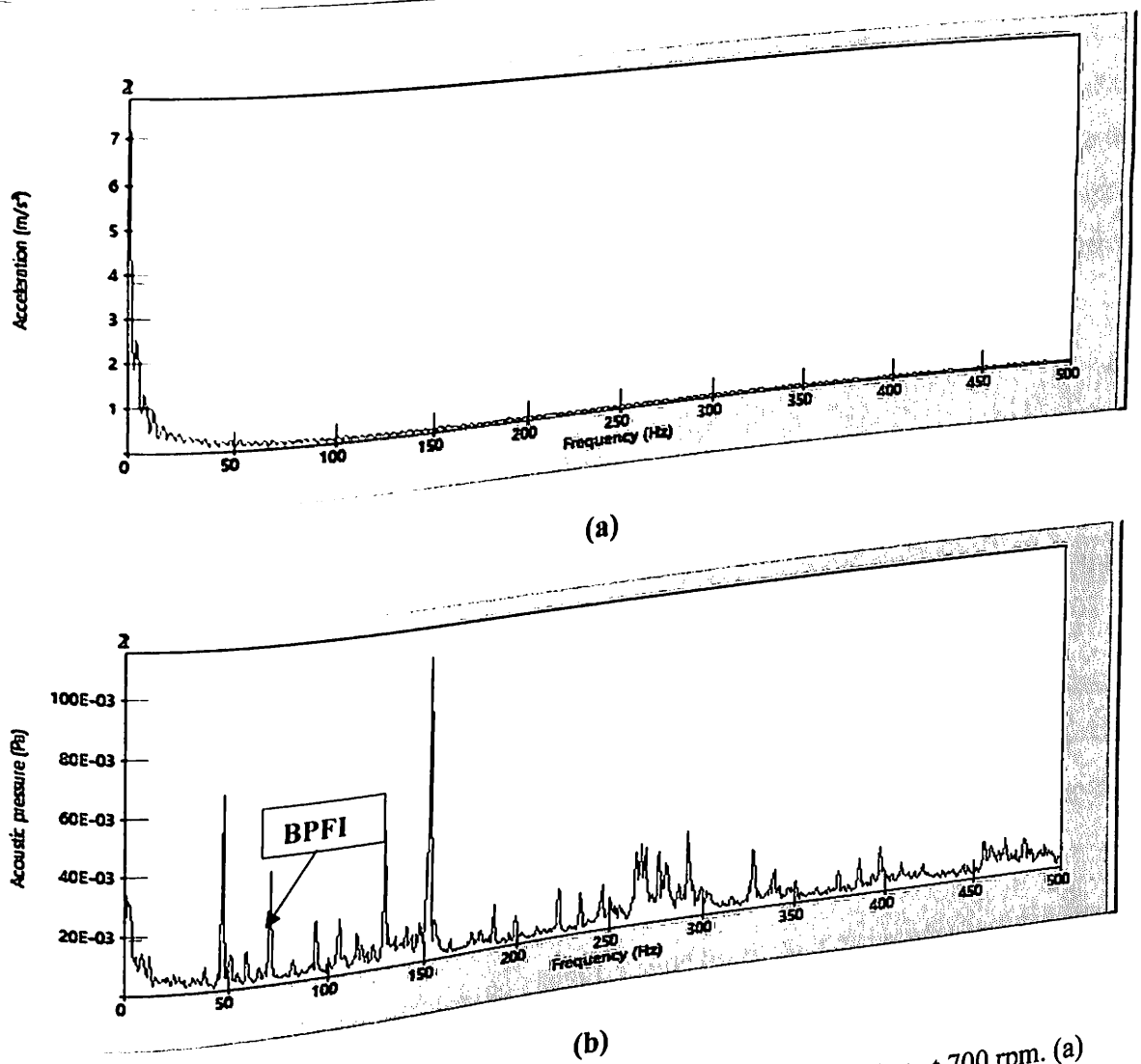

Figure 6.10 Vibro-Acoustic FFT of Ball defect and Inner race defect at 700 rpm. (a) Vibration FFT. (b) AE FFT.

6.5 Conclusion

Fusion of multiple sensors for condition monitoring of bearing intended to provide more information than individual sensors. Enhancement of fault detection and diagnosis occurs due to data fusion from different sensors, by obtaining supportive information.

In this chapter, an intelligent fault diagnosis system was proposed to predict and diagnose bearing failures using two sensors: Accelerometer and Microphone. These two sensors create a fusion called as vibro-acoustic. This system adopts waterfall fusion model as a

fusion technique for optimally combining sensor data, to attain the best decisions upon overall health conditions of bearing components. Six cases of bearing health conditions were tested using the proposed methodology, and its results were compared with the result obtained from individual sensors based on conventional methods. The result concludes that, the outcome proves the benefit of the proposed method for enhancing fault detection and provide the basis for prognosis of bearing.

References

1] Tandon, N., & Choudhury, A. (1999). A review of vibration and acoustic measurement methods for the detection of defects in rolling element bearings. Tribology international, 32(8), pp.469-480.

2] N.S.Feng, E.J.Hahn, R.B.Randall (2002), Using transient analysis software to simulate vibration signals due to rolling element bearing defects, Proceedings of the Third Australian Congress on Applied Mechanics, Sydney, New South Wales, Australia,pp.689–694.

3] Jalan, A.K. and Mohanty, A.R., (2009). Model based fault diagnosis of a rotor–bearing system for misalignment and unbalance under steady-state condition. Journal of Sound and Vibration, 327(3-5), pp.604-622.

4] Rafsanjani, A. et al. (2009) 'Nonlinear dynamic modeling of surface defects in rolling element bearing systems',319, pp.1150-1174.

5] Hecke, B. Van, Yoon, J. and He, D. (2016) 'Low speed bearing fault diagnosis using acoustic emission sensors,' Applied acoustics. Elsevier Ltd, 105, pp. 35–44. doi: 10.1016/j.apacoust.2015.10.028.

6] Al-ghamd, A. M. and Mba, D. (2006) 'A comparative experimental study on the use of acoustic emission and vibration analysis for bearing defect identification and estimation of defect size', 20, pp. 1537–1571. doi: 10.1016/j.ymssp.2004.10.013.

7] Elforjani, M. and Mba, D., (2010). Accelerated natural fault diagnosis in slow speed bearings with acoustic emission. Engineering Fracture Mechanics, 77(1), pp.112-127.

8] El-Thalji, I. and Jantunen, E., (2015). A summary of fault modelling and predictive health monitoring of rolling element bearings. Mechanical systems and signal processing, 60, pp.252-272.

9] Heng, A., Zhang, S., Tan, A.C. and Mathew, J., (2009). Rotating machinery prognostics: State of the art, challenges and opportunities. Mechanical systems and signal processing, 23(3), pp.724-739.

10] Liu, Z., Cao, H., Chen, X., He, Z. and Shen, Z., (2013). Multi-fault classification based on wavelet SVM with PSO algorithm to analyze vibration signals from rolling element bearings. Neurocomputing, 99, pp.399-410.

11] Chen, Z., Deng, S., Chen, X., Li, C., Sanchez, R.V. and Qin, H. (2017). Deep neural networks-based rolling bearing fault diagnosis. Microelectronics Reliability, 75, pp.327-333.

12] Abbasion, S., Rafsanjani, A., Farshidianfar, A. and Irani, N., (2007). Rolling element bearings multi-fault classification based on the wavelet denoising and support vector machine. Mechanical Systems and Signal Processing, 21(7), pp.2933-2945.

13] Seera, M., Wong, M.D. and Nandi, A.K., (2017). Classification of ball bearing faults using a hybrid intelligent model. Applied Soft Computing, 57, pp.427-435.

14] B.Li, M.YuenChow, Y.Tipsuwan, J.C.Hung,(2000) Neural-network-based motor rolling bearing fault diagnosis, IEEE Trans.Ind.Electron. 47(5), pp.1060–1069.

15] Samanta, B. and Al-Balushi, K.R., (2003). Artificial neural network-based fault diagnostics of rolling element bearings using time-domain features. Mechanical systems and signal processing, 17(2), pp.317-328.

16] Gryllias, K.C. and Antoniadis, I.A., (2012). A Support Vector Machine approach based on physical model training for rolling element bearing fault detection in industrial environments. Engineering Applications of Artificial Intelligence, 25(2), pp.326-344.

17] L. Guo, J.Chen, X.i.Li, (2009), Rolling bearing fault classification based on envelope spectrum and support vector machine ,Journal of Vibration Control 15(9) pp. 1349–1363.

18] Safizadeh, M.S. and Latifi, S.K., (2014). Using multi-sensor data fusion for vibration fault diagnosis of rolling element bearings by accelerometer and load cell. Information Fusion, 18, pp.1-8.

19] C.Sujatha, Vibration and Acoustics: Measurement and signal analysis, Published by Tata Megraw Hill Education Private Limited, New Delhi, India.(2010).